Food Sci Biotechnol (2020) 29(7):927–937
https://doi.org/10.1007/s10068-020-00745-3

Effects of pigment and citrinin biosynthesis on the metabolism and morphology of *Monascus purpureus* in submerged fermentation

Xueying Chai[1,2] · Zhilu Ai[1] · Jun Liu[1,2] · Ting Guo[2] · Jingyan Wu[2] · Jie Bai[2] · Qinlu Lin[2]

Received: 18 July 2019 / Revised: 7 February 2020 / Accepted: 28 February 2020 / Published online: 30 March 2020

Abstract The effects of the secondary metabolite biosynthesis on the metabolism and morphology of the *Monascus purpureus* were investigated in this study. Hypha and septum length became longer after deletion of genes *pig*R and *pks*CT in *M. purpureus* LQ-6 by *Agrobacterium tumefaciens*-mediated transformation technology, highly branched hyphae, much smaller and freely dispersed mycelial pellets were observed in *M. purpureus*. Compared with that in the wild-type, the level of intracellular NADH and NADPH was almost constant in *M. purpureus* Δ*pig*R at 4 days, but the NADH and NADPH levels decreased by 1.58-fold and 3.71-fold in *M. purpureus* Δ*pks*CT. The present study can not only provide a kind of strategy to improve the *Monascus* pigments production, but also provide theoretical support for the further study of relationship between the secondary metabolites, metabolism and morphological change.

Keywords *M. purpureus* · *pig*R · *pks*CT · Morphology · Cofactor

Introduction

The fungus *Monascus* spp. has been well-known in many oriental countries for centuries, especially in China, Japan, and Korea. *Monascus* spp. is conventionally cultured on steamed white polished rice to produce a fermented meal known as red mold rice (RMR) in the USA, Hongqu in China, and Koji and Red Koji in Japan. There are hundreds of scientific studies that indicate that RMR contains many kinds of beneficial compounds, such as natural pigments (used as food colorants), monacolin K or lovastain (HMG-CoA reductase inhibitor), and gamma-amino butyric acid (GABA, a kind of hypotensive agent) (Patakova, 2013; Shao et al., 2014). However, the usage of RMR also incurs controversy since the discovery of citrinin (a kind of mycotoxin, shown to be nephrotoxic in animals) production by *Monascus* strains. Although there are no strict rules limiting the upper amount of citrinin in RMR in China, a

Electronic supplementary material The online version of this article (https://doi.org/10.1007/s10068-020-00745-3) contains supplementary material, which is available to authorized users.

✉ Qinlu Lin
linqinlu@hotmail.com

Xueying Chai
xueyingchai@outlook.com

Zhilu Ai
zhila@163.com

Jun Liu
liujundandy@126.com

Ting Guo
guoting@hotmail.com

Jingyan Wu
609226894@qq.com

Jie Bai
474445729@qq.com

[1] Key Laboratory of Staple Grain Processing, Ministry of Agriculture and Rural Affairs of the People's Republic of China, Zhengzhou 450002, Henan, China

[2] National Engineering Laboratory for Deep Process of Rice and Byproducts, Hunan Key Laboratory of Grain-oil Deep Process and Quality Control, Hunan Key Laboratory of Processed Food for Special Medical Purpose, College of Food Science and Engineering, Central South University of Forestry and Technology, Changsha 41004, Hunan, China

limit of 2000 ppb (2000 μg/Kg) in RMR was established in Europe according to UC Commission regulation No. 212/2014, 50 ppb in South Korea (Kim et al., 2007), and 200 ppb in Japan (Fu et al., 2007). However, according to Chinese National Standard GB 1886.181-2016, the upper limit of citrinin was determined to be 0.04 ppm/U in MPs.

Pigments, monacolin K, and citrinin are the three most famous polyketide (PK) secondary metabolites produced by filamentous fungi *Monascus* strains, which were catalyzed by polyketide synthase, composed of catalytic domains consisting of ketosynthase (KS), acyltransferase (AT), product template (PT), acyl carrier protein (ACP), and C-methyltranferase (MT) (Balakrishnan et al., 2013). MPs are a mixture of azaphilones mainly composed of yellow pigments (ankaflavin and monascin), orange pigments (monascorubrin and rubropunctatin), and red pigments (monascorubramine and rubropunctamine) (Kim and Ku 2018; Wang et al., 2015), and the related metabolic pathway showed that yellow pigments are formed from orange pigments by reduction, and the orange colors could convert into red when oxygen atoms are replaced by an amino group.

One of the main challenges in the production of fungal metabolites by filamentous fungi such as *Monascus* is the control of mycelial morphology, which attached great importance to the production of metabolites (Lv et al., 2017). Hyphae of filamentous fungi in submerged batch-fermentation (SBF) mainly exist in three different morphology, including free mycelia, mycelial pellets mycelial clumps (Zhang et al., 2015). Filamentous fungi morphology are much affected by fermentation conditions and genetic factors, such as pH, shaking speed (Ibrahim, 2015; Lv et al., 2017), oxygen diffusion (Vecht-Lifshitz et al., 1990), exogenous additive such as cyclic AMP (Lai et al., 2011) and nonionic surfactant Triton X-100 (Chen et al., 2018). The nonionic surfactants were correlated with pigment production and morphology in SBF, which resulted in a higher level of MPs production and changed the mycelia morphology (Yang et al., 2019). In the production of *Monascus* red pigment, the maximum production of MPs was obtained with high agitation rates, and shorter branches were produced in *Monascus* mycelium (Kim et al., 2002). To note, many scholars have studied the relationship between mycelial morphology and pigment, but whether the effect of citrinin biosynthesis on mycelial morphology is the same as that of pigment has not been investigated. Furthermore, the effects of pigment synthesis and citrinin metabolism on *Monascus* metabolism such as cofactor metabolism are still unclear.

It is well-known that three secondary metabolites—pigments, monacolin K, and citrinin—share a biosynthetic pathway before a certain branch point, synthesized by acetyl CoA and malonyl-CoA, especially for pigment and citrinin (Fig. 1). Although many researchers have found that disruption of citrinin or monacolin K biosynthesis could increase the production of pigment, the relationship between the secondary metabolite biosynthesis and other intracellular metabolism (such as the glycolysis pathway and cofactor generation) and the effect of the secondary metabolites on the cell growth and morphology and physiology of hypha are still unclear. Hence, the aim of this work was to investigate the effect of the secondary metabolite biosynthesis on the metabolism and morpholog of the *M. purpureus* strain by disruption of the biosynthetic pathway of pigments and citrinin using *Agrobacterium tumefaciens*-mediated transformation (ATMT) technology.

Materials and methods

Microorganisms, cultivation, and materials

Monascus purpureus LQ-6 (CCTCC M 2018600, China Central for Type Culture Collection (CCTCC), Wuhan, China), as the parent strain, was isolated from red mold rice obtained from a market in China. *M. purpureus* strains were cultured on potato dextrose agar (PDA, potato (200 g), dextrose (20 g), and agar (20 g) in 1000 mL pure water) medium with the addition of 50 μg/mL hygromycin or G418 as required at 30 °C. *Escherichia coli* DH5α cells were grown in Luria–Bertani (LB, tryptone (10 g/L), yeast extract (5 g/L), NaCl (10 g/L)) medium or solid medium (addition of 20 g/L agar) with the addition of 50 μg/mL kanamycin as required at 37 °C. The strains and plasmids used in this study are listed in Table S1.

Construction of *pig*R and *pks*CT deletion vector

As shown in Fig. S1, homologous recombination was applied for knocking out the *pig*R gene in *M. purpureus* LQ-6. The primers used in this study are listed in Table S2. There are two steps to construct the *pig*R disruption vector, as follows.

To construct the *pig*R-deleted cassette, a 1.54 kb 5′ homologous arm and a 1.53 kb 3′ homologous arm (named 5′-UTR and 3′-UTR, respectively) were amplified from *M. purpureus* LQ-6 genomic DNA by the polymerase chain reaction (PCR) using the primers *pig*R-up-R, *pig*R-up-F, and *pig*R-dn-R, *pig*R-up-F, respectively. A 2.1 kb fragment containing the G418 gene from the plasmid pXS (the primers G418-R, G418-F) was fused with 5′-UTR and 3′-UTR by overlap PCR to generate the *pig*R-deleted cassette (Ning et al., 2017).

The *pig*R-deleted cassette obtained from the first step was cloned into the corresponding sites of the pCAMBIA3300 binary vector linearized by double digestion with

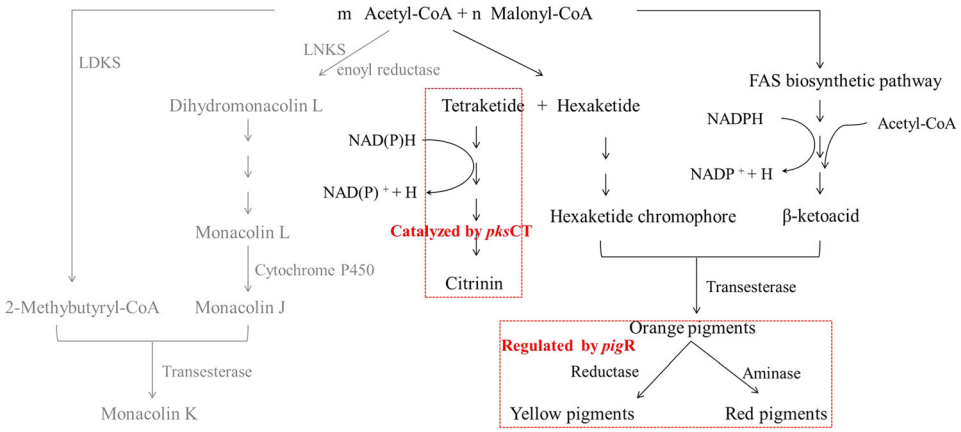

Fig. 1 The biosynthetic pathway of secondary metabolite pigment, citrinin, and monacolin K in *M. purpureus*

EcoR I and *Hind* III using a one-step cloning kit (Vazyme Biotech Inc., Nanjing, China). Finally, the *pig*R deletion vector named pCAMBIA3300-Δ*pig*R was formed(Xie et al., 2013).

To construct the *pks*CT disruption vector, a similar strategy as above was used. In addition, the selection marker for *pks*CT was *hph*, which was amplified from the plasmid pAN7-1with a primer pair *hph*-F and *hph*-R.

Transformation of *M. purpureus*

ATMT technology was used to transform the disruption vector, according to Shao et al.(Shao et al., 2009). *M. purpureus* LQ-6 was cultured on a Potato Dextrose Agar (PDA) plate for 10 days at 30 °C, and then 5 mL of sterile water was added to the PDA plate with a fully-grown culture of *M. purpureus* LQ-6. The suspension was filtered through two layers of sterile lens paper to collect the spores. Then, *A. tumefaciens* EHA105 containing recombinant plasmid pCAMBIA3300-ΔpigR was inoculated for 2 days at 28 °C in minimal medium (2 g/L glucose, 2.05 g/L K_2HPO_4, 1.45 g/L KH_2PO_4, 0.01 g/L $CaCl_2$, 0.6 g/L $MgSO_4$, 0.3 g/L NaCl, 0.5 g/L $(NH_4)_2SO_4$, pH = 7.0, supplemented with 10 mL 0.01% (v/v) $FeSO_4$) supplemented with kanamycin (50 μg/mL). After dilution to an optical density (OD) of 0.15 at 600 nm with induction medium (2 g/L glucose, 1.84 g/L K_2HPO_4, 1.45 g/L KH_2PO_4, 0.01 g/L $CaCl_2$, 0.6 g/L $MgSO_4$, 0.3 g/L NaCl, 0.5 g/L $(NH_4)_2SO_4$, 5 g/L glycerol, pH = 4.9, supplemented with 10 mL 0.01% $FeSO_4$, 10 mL 100 g/L MES (pH 5.5), and 5 mL 200 mM acetosyringone), the cell suspension of *A. tumefaciens* EHA105 needed an additional 6 h growth under the same conditions. Next, the *A. tumefaciens* cell suspension was mixed with spore pellets of *M. purpureus* LQ-6 at a concentration of 10^6 spores/mL, and the mixture (200 μL) was plated on the coculture-inducing medium (1 g/L glucose, 1.84 g/L K_2HPO_4, 1.45 g/L KH_2PO_4, 0.01 g/L $CaCl_2$, 0.6 g/L $MgSO_4$, 0.3 g/L NaCl, 0.5 g/L $(NH_4)_2SO_4$, 5 g/L glycerol, 20 g/L agar, supplemented with 10 mL 0.01% (v/v) $FeSO_4$, 10 mL 100 g/L MES (pH 5.5), and 10 mL 200 mM acetosyringone) covered with cellophane. After co-cultivation for 4 days at 25 °C, the cellophane was removed, and an empty sterile culture dish with poured PDA containing 50 μg/mL G418 for selecting transformants and 200 μg/mL cephalosporin for killing the *A. tumefaciens* cells was used. Following cultivation for 2 days at 25 °C, single colonies were picked up and cultured on PDA supplemented with G418. If these colonies still grew on the selective medium, they were regarded as transformants.

For deletion of gene *pks*CT (50 μg/mL hygromycin as the selection agent) and double deletion of genes *pig*R and *pks*CT (disruption of gene *pks*CT in the background of recombinant stain *M. purpureus* Δ*pig*R), the same method described above was performed.

Confirmation of recombination strains

After *Agrobacterium tumefaciens*-mediated transformation of the disruption vectors, PCR analysis was subjected to identify transformants. For PCR analysis, genomic DNA was isolated from transformant mycelia using the CTAB method(Shao et al., 2009). Primers *pig*R-T-F/R, pigR-half-F, and G418-T-R were used to confirm the deletion fragment of *pig*R and the double deletion fragment of *pig*R and *pks*CT. The deletion fragment in the genomic DNA of the hygromycin-resistant transformants was amplified using primers CT-T-F/R, CT-half-F, and hyh-T-R. The recombinant strains were named *M. purpureus* ΔpigR (*pig*R-deleted strain), *M. purpureus* Δ*pks*CT (*pks*CT-deleted strain), and *M. purpureus* Δ*pks*CT:*pig*R (*pig*R and *pks*CT-double deleted strain), respectively.

Submerged batch-fermentation

Sterile water (10 mL) was added to the PDA medium with a fully-grown culture of *M. purpureus* and aseptically scraped using a sterile inoculating loop to obtain a spore suspension. For SBF, 5 mL of the spore suspension (10^6 spores/mL) was inoculated into 45 mL liquid-state fermentation medium in 250 mL conical flasks at 30 °C while shaking at 150 rpm in the dark for 252 h (Liu et al., 2019; Terán et al., 2018). Fermentation kinetics assays were conducted in 1000 mL conical flasks containing 200 mL SBF medium.

Image analysis

For the physiological characteristics assay, a 5 μL spore suspension was inoculated into the middle of a PDA plate (diameter = 90 mm) at 30 °C to analyze the colony size and spore development rate. For 5 days, SBF samples were taken to observe the morphology of mycelial pellets. All of them were monitored by a digital camera (Canon EOS 80D, Japan).

For the microscopy assay, the hyphae of strains were taken using a sterile inoculating loop from the cultured PDA plate for 3 and 5 days, respectively. Afterwards, the hyphae were re-suspended in sterile water and imaged using a Motic compound microscope (BA200, Germany).

Metabolites analytic methods and calculation

The fermentation broth was centrifuged at 8000 rpm for 10 min to collect mycelia and supernatant, respectively. For total biomass determination, the collected mycelia were washed three times with distilled water and dried at 60 °C. The total biomass concentration was expressed as dry cell weight (DCW) per unit volume of fermentation medium. The supernatant was diluted to measure the residual glucose concentration using the standard 3,5-dinitrosalicylic acid (DNS) method. After SBF finished, the collected mycelia were soaked in 5 volumes of 70% (v/v) ethanol at 60 °C for 2 h for determination of the intracellular pigment production. The fermentation supernatant was directly measured for analysis of extracellular pigments. The concentration of MPs was analyzed by measuring the corresponding absorbance by a UV–visible spectrophotometer (UV-752 N), at 505 nm for red pigments, 470 nm for orange pigments and 420 nm for yellow pigments, respectively. The total MPs concentrations include intracellular pigment production and exMPs production (Chen et al., 2017).

For analysis of monacolin K and citrinin production, 5 mL of the fermentation medium was inoculated into 20 mL of 75% (v/v) methanol at 60 °C for 2 h, followed by cooling to room temperature and allowing to settle overnight. After centrifuging at 10,000 rpm for 5 min and filtering through a 0.22 μm filter, the supernatant was assessed by high performance liquid chromatography (HPLC, LC-30A, Shimadzu) on a reverse phase C_{18} column (5 μm, 150 × 4.6 mm) (Zhang et al., 2017). Monacolin K production was determined with methanol/water (70:30, pH adjusted to 3 with orthophosphoric acid) as the mobile phase, 1.0 mL/min flow rate at 25 °C, and 10 μL injection volume, and the eluate was monitored by a UV detector at a wavelength of 237 nm(Lin et al., 2018). To determine the concentration of citrinin, a mixture of acetonitrile, isopropanol, and 0.08 mol/L orthophosphoric acid at a ratio of 35:10:55 (v/v) as the mobile phase, with a 1.0 mL/min flow rate at 25 °C and injection volume of 10 μL was examined using a fluorescence detector (Prominence RF-20A/20Axs) at a 331 nm excitation wavelength and 500 nm emission wavelength (according to the Chinese National Standard GB 5009.222-2016).

Intracellular concentrations of NADH and NADPH were detected via Amplite™ Colorimetric NAD/NADH and NADP/NADPH Assay Kits (Beijing Solarbio Science & Technology Co., Ltd., China). Mycelium were taken from the batch-fermentation and then rapidly ground into a powder using liquid nitrogen. The mycelium powder (0.1 g, wet weight) was transferred quickly into a sample tube for measurement(Huang et al., 2017).

Each experiment was repeated at least three times. Numerical data are presented as the mean ± standard deviation (SD).

Accession numbers

The genome sequences have been deposited into the NCBI database with an accession number of PRJNA503091.

Results and discussion

Sequence determination and bioinformatics analysis

There are many kinds of *Monascus*, including *M. ruber*, *M. purpureus*, *M. fuliginosus, M. aurantiacus, M. pilosus* and so on. To determine the species, strain LQ-6 isolated naturally was identified by ITS4/5. After purification of the PCR product, the ITS fragment of strain LQ-6 was sequenced and was homologous to multiple strains of *Monascus*, especially *M. purpureus*. Furthermore, the phylogenetic tree by selecting strains with high homology and other strains of the same genus was constructed (Fig. 2A). The phylogenetic tree indicated that the strain LQ-6 (named unk in Fig. 2A) displayed high homologies with *M. purpureus*, *M. ruber*, *M. pilosus*, and *M.*

fuliginosus, especially *M. purpureus* Z1 (97% query cover and 99.77% identity from NCBI-BLASTN). The strain LQ-6 was named as *M. purpureus* LQ-6.

Gene *pig*R, is a pathway-specific regulatory gene for MPs biosynthesis, which is of great significance in MPs biosynthesis pathway(Xie et al., 2013). Gene *pks*CT is highly correlated with citrinin production, which is polyketide synthase gene responsible for citrinin biosynthesis (Shimizu et al., 2005). In this study, whole genome sequencing was performed to unearth gene *pig*R and *pks*CT in *M. purpureus* LQ-6, and the biosynthetic pathway of pigment and citrinin was blocked by disrupting the gene *pig*R and *pks*CT, respectively. Genes *monacsus_3525* and *monacsus_3836* were unearthed after sequencing the whole genome of *M. purpureus* LQ-6 and showed significant similarity to *pig*R and *pks*CT, respectively. The nucleotide sequence of gene *monacsus_3525* was 3634 bp in length and encoded by 573 amino acids. A database search with NCBI-BLASTP suggested that it has 92.48% similarity with the pigment biosynthesis activator *pig*R (encoded by 554 amino acids) of the pigment biosynthesis cluster from *Monascus ruber* M7 (protein ID = AGL44390.1). Based on the results of NCBI-BLASTP, the phylogenetic tree of gene *monacsus_3525* was constructed. It demonstrated that the gene *monacsus_3525* displayed high homologies with *pig*R in *M. ruber* (query cover = 100%, identity = 92.48%, bootstrap value = 78), pigment biosynthesis gene cluster in *M. pilosus*, and then citrinin biosynthetic gene cluster in *M. ruber* (identity = 46.10%) (Fig. 2B). In addition, there was almost no pigment produced after deletion of gene *Monascus_3525* (Figs. 3 and 5C). Gene *pks*CT was highly conserved in different citrinin-producing *Monascus* strains (Chen et al., 2008; Fu et al., 2007), encoding polyketide synthase, which is responsible for citrinin biosynthesis (Jia et al., 2010). The nucleotide acid sequence of gene *monacsus_3836* was used as a query to perform BLASTN in the NCBI database. The results revealed that gene *monacsus_3836* had 100% similarity to the gene *pks*CT from *M. purpureus* (sequence ID: AB167465.1) (Fig. S2). Furthermore, deletion of the gene *Monascus_3836* in *M. purpureus* LQ-6 resulted in no citrinin production (Fig. S4). The above results and analysis indicate that the genes *Monascus_3525* (*pig*R) and *monscsus_3836* (*pks*CT)

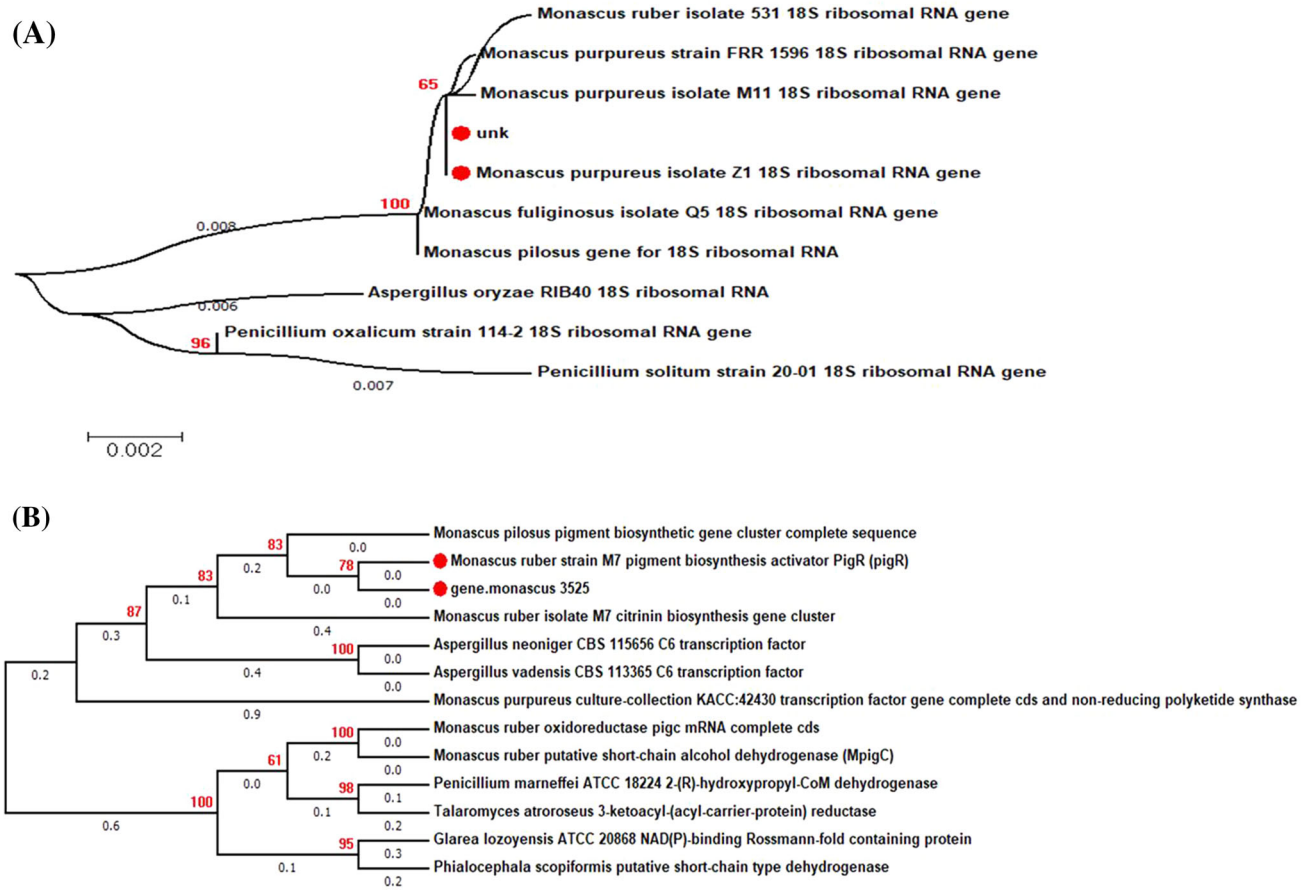

Fig. 2 Phylogenetic tree obtained by neighbor-joining based on ITS gene sequences of strain LQ-6 (marked as unk) (A) and amino acid sequence of gene *Monascus*_3525. (B). Numbers in red above branches indicate bootstrap values

play a vital role in pigment and citrinin biosynthesis of *M. purpureus* LQ-6, respectively.

However, there was no monacolin K (acid form and lactone form) produced by solid-state fermentation using *M. purpureus* LQ-6 (Fig. S5). It has been reported that some *M. purpureus* strains lack the monacolin K synthesis locus and are incapable of producing monacolin K (Kwon et al., 2016). Then, it's speculated that the monacolin K biosynthetic gene cluster in *M. purpureus* LQ-6 was incomplete or lacking. The results of whole genome sequencing of *M. purpureus* LQ-6 showed that just genes *Monascus_1765*, *Monascus_1766*, *Monascus_1767*, *Monascus_1768*, *Monascus_1769*, *Monascus_1770*, and *Monascus_1771* were located in the monacolin K biosynthetic gene cluster, and the protein homology was low, except for *Monascus_1766* with 83.78% identity to the protein mkC and *Monascus_1765* with 74.49% identity to the protein mkB from *Monascus pilosus* by BLASTP analysis. Through sequence analysis and solid-state fermentation, it's concluded that there was no monacolin K produced by *M. purpureus* LQ-6, resulting from the biosynthetic gene cluster being incomplete. In addition, different strains of *Monascus* should be selected to study different secondary metabolites. Generally, *Monascus*

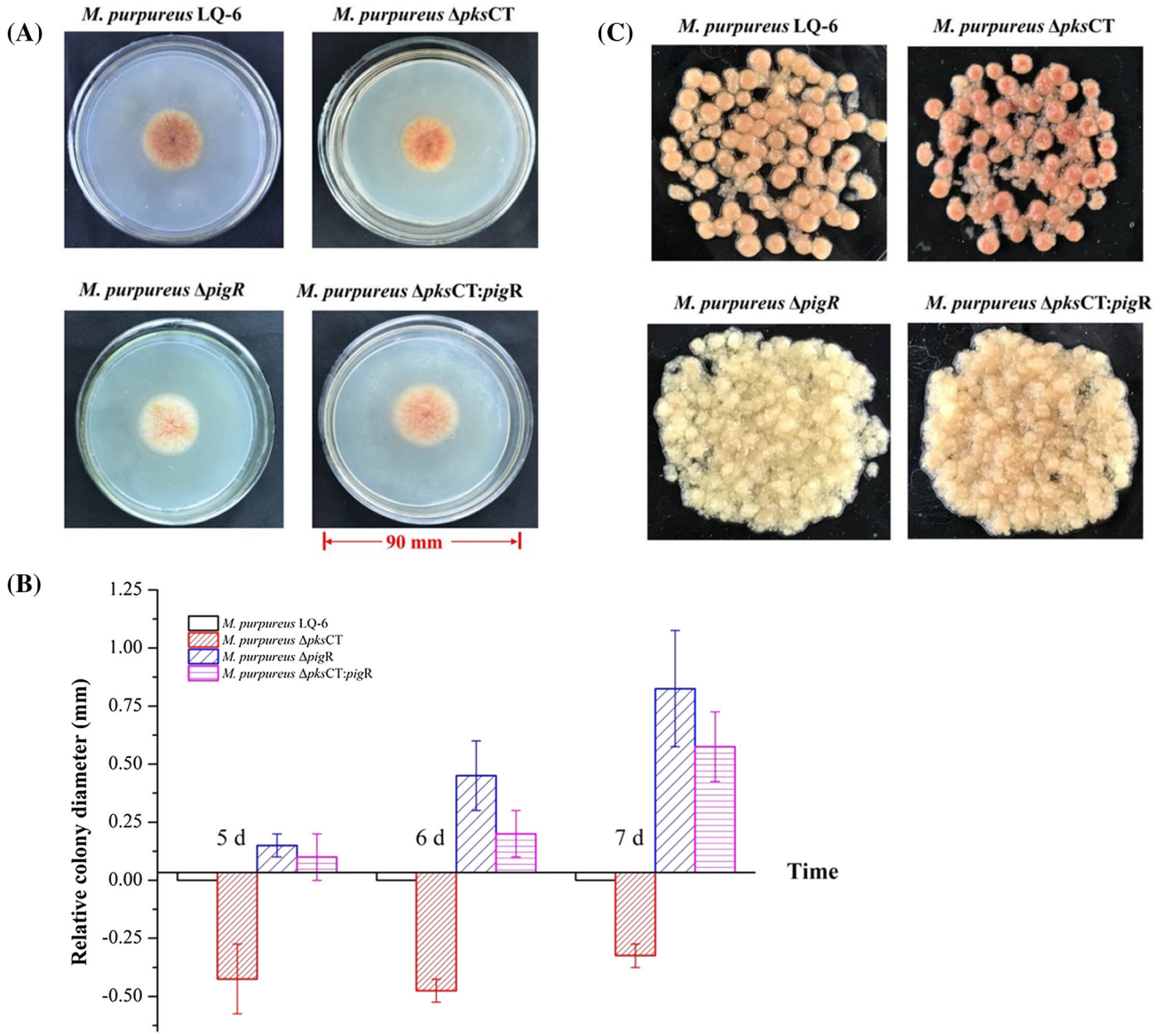

Fig. 3 Colonial morphologies of wild-type strain *M. purpureus* LQ-6 and recombination strains cultivated on PDA plates at 30 °C for 5 days (A). Relative colony diameter of different strains cultivated on PDA plates on the 5th, 6th, and 7th days, with the colony diameter of *M. purpureus* LQ-6 as a reference (B). Mycelial morphologies of *M. purpureus* LQ-6 and recombination strains fermented at 150 rpm for 5 days in SBF medium (C)

fuliginosus, Monascus ruber and *Monascus pilosus* are considered to have strong production capacity of monacolin K, which were often used in monacolin K related research. *M. purpureus* has strong ability of producing pigment, but also with citrinin. Furthermore, given that many researches focus on the aspect of food safety to decrease the citrinin production by *M. purpureus* fermentation, then this strain LQ-6 was finally engineered. Besides, this study mainly focus on the morphology and metabolism in submerged fermentation after disrupting pigment and citrinin biosynthesis pathways.

Effect of biosynthesis of pigment and citrinin on morphology of *M. purpureus* LQ-6

In SBF, the production of secondary metabolites is strongly associated with the fungal morphology and growth (Chen et al., 2018; Sun et al., 2018). We speculated that disruption of the biosynthetic pathways of pigments and citrinin would change the development and cellar morphology in *M. purpureus* LQ-6. In this study, the changes in spore development, hyphal length and branching, and mycelial pellet morphology were analyzed. The colony phenotypes of LQ-6 and recombination strains incubated on PDA at 30 °C for 5 days are shown (Fig. 3A), and the order of spore germination rate was *M. purpureus* Δ*pig*R, *M. purpureus* Δ*pks*CT:*pig*R, *M. purpureus* LQ-6, and *M. purpureus* Δ*pks*CT. In addition, the hyphae of *M. purpureus* Δ*pig*R and *M. purpureus* Δ*pks*CT:*pig*R were white, which resulted from blocking the pigment biosynthesis pathway after deletion of gene *pig*R. Lv et al. have been reported the hyphal diameter was highly correlated with the biosynthesis of the MPs (Lv et al., 2017). The colony diameter of LQ-6, Δ*pks*CT, Δ*pig*R and Δ*pks*CT:*pig*R was 31.75, 27.50, 33.25and 32.75 mm, respectively. During the process of cultivation, the diameter of *M. purpureus* Δ*pks*CT was smaller than that of the wild-type strain, but the diameters of *M. purpureus* Δ*pig*R and *M. purpureus* Δ*pks*CT:*pig*R were bigger than that of the wild-type strain, and the differences in colony diameter were more obvious with the development of culture process (Fig. 3B). These phenomena illustrated that the genes *pig*R and *pks*CT have a great impact on spore germination and development, and blocking pigment biosynthesis can increase the cell growth rate, whereas it is reduced after disrupting citrinin biosynthesis. After the *pig*R gene was knocked out, the growth of *Monascus* did not inhibited, and the growth rate was higher than that of the parental strain LQ-6, indicating that the *pig*R gene was not involved in the primary metabolism synthesis, only related to MPs biosynthesis. Based on aboved results, observing the mycelial morphology and the measuring hyphal diameter can preliminary predict the production of *Monascus* secondary metabolites.

In SBF, two main morphologies were observed, including pellets and free mycelium. In addition, the morphology of filamentous fungi in SBF plays a significant role in metabolites yield as well as productivity (Ibrahim, 2015). In this study, mycelial pellets were formed by development from the spores and hyphae of the wild-type strain LQ-6 at 150 rpm for 5 days in SBF medium, as well as *M. purpureus* Δ*pks*CT, except the surface color of the pellets was redder (Fig. 3C). However, compared to the mycelial pellets of the wild-type strain, they were much smaller and more freely dispersed in the liquid fermentation medium after deletion of gene *pig*R in *M. purpureus* LQ-6. Furthermore, the number of cleistothecium (seen at 3 days) and hypha length (seen at 5 days) of *M. purpureus* were both increased by deletion of genes *pig*R and *pks*CT, especially in *M. purpureus* Δ*pks*CT (Fig. 4). Additionally, the septum of hypha became longer in *M. purpureus* Δ*pks*CT and *M. purpureus* Δ*pig*R than that in the wild-type strain. It reported that the extent of increase of hyphae branches was used as an indicator of the cell growth rate of the fungi (Papagianni, 2004). In this study, highly branched hyphae were observed in *M. purpureus* Δ*pig*R but did not appear in *M. purpureus* Δ*pks*CT, which was consistent with the above-mentioned results. There may be competitive utilization of some nutrients in the biosynthesis of MPs and the growth of *Monascus*, which leads to the inhibition of pigments biosynthesis on the growth of *Monascus*. These findings revealed that not only changing the morphology of *Monascus* can affect the pigments yield, but also blocking the synthesis of pigment and citrinin can affect the morphology and growth rate of *M. purpureus*.

Effect of biosynthesis of pigment and citrinin on the metabolism of *M. purpureus* LQ-6

To evaluate the effect of pigments and citrinin biosynthesis on the metabolism of *M. purpureus*, the corresponding biosynthetic pathways were disrupted by deletion of genes *pig*R and *pks*CT. From the analysis of fermentation kinetics of various strains (Fig. 5), the recombination strains (*M. purpureus* Δ*pig*R, *M. purpureus* Δ*pks*CT, and *M. purpureus* Δ*pks*CT:*pig*R) showed a higher glucose consumption rate compared to the wild-type strain *M. purpureus* LQ-6 at the fermentation prophase, especially *M. purpureus* Δ*pig*R. In addition, the wild-type strain showed a long lag phase (glucose consumption rate was 0.10 g/L h for 36 h), which did not appear in the fermentation kinetics of the three recombination strains with a similar glucose consumption rate (Fig. 5A). These results revealed that deletion of genes *pig*R and *pks*CT can reduce the fermentation lag phase in *M. purpureus* LQ-6. In addition, investigation of the cell growth coupled with the glucose consumption in the fermentation process (Fig. 5B) showed

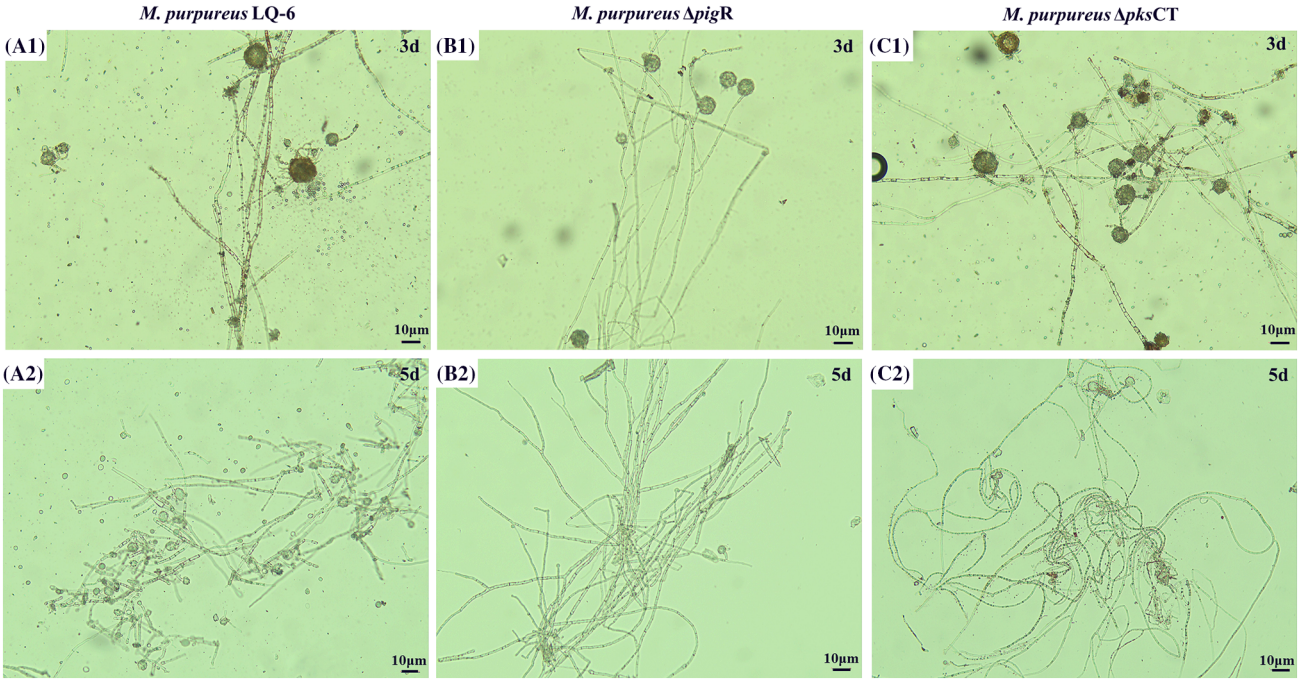

Fig. 4 The morphology of the hyphae of *M. purpureus* LQ-6 (A), *M. purpureus* Δ*pig*R (B), and *M. purpureus* Δ*pks*CT (C) cultivated on PDA plates at the 3th and 5th days

that the cell growth rate slightly increased after deletion of gene *pig*R and double knockout of genes *pig*R and *pks*CT, which resulted in 1.04-fold and 1.02-fold times the DCW of the wild-type, respectively. However, the *pks*CT-deleted

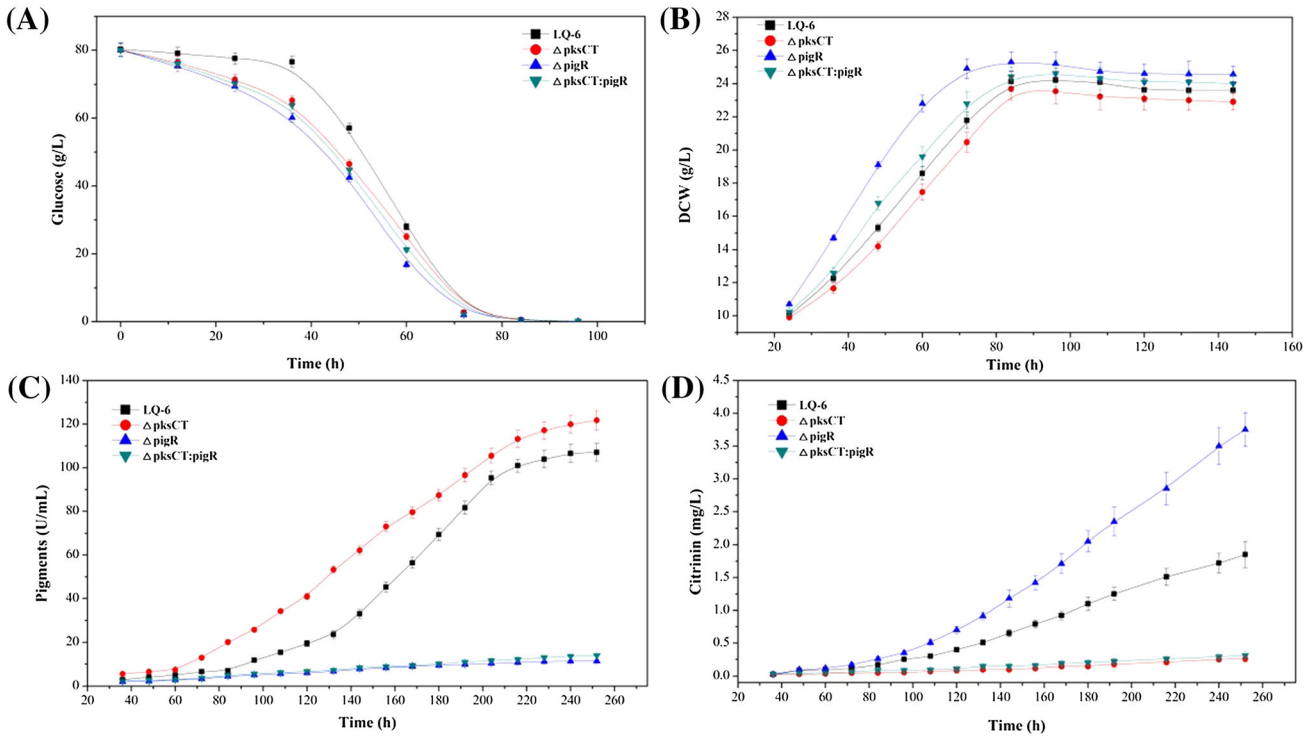

Fig. 5 Submerged batch-fermentation kinetics of *M. purpureus* LQ-6 and recombination strains. Glucose consumption (A), cell growth (B), pigment production (C), and citrinin production (D). Submerged batch-fermentations were studied in 1000 mL conical flasks containing 200 mL SBF medium at 150 rpm in the dark for 252 h

strain decreased to 1.04-fold times the DCW of the wild-type and a lower cell growth rate. It's speculated that the synthesis of MPs can affect the growth and glucose consumption of *Monascus* spp., which is consistent with a previous study (Xie et al., 2015).

The secondary metabolites biosynthesis pathway is described in Fig. 1. The monacolin K biosynthesis pathway was incomplete because of the lack of one or more key genes in the gene clusters in *M. purpureus* LQ-6; gene *pig*R-regulated pigments biosynthesis and gene *pks*CT catalyze citrinin production. Xie et al. reported the production of citrinin was dramatically improved by 1.60-fold after deletion of the gene *pig*R (Xie et al., 2013). In addition, blocking of the production of citrinin resulted in 40% more pigment in *M. aurantiacus* Li AS3.4384 (Ning et al., 2017). Similarly, deletion of gene *pks*CT in *M. aurantiacus* resulted in significantly decreased citrinin production. Furthermore, this Δ*pks*CT mutant exhibited a stronger ability to produce red and yellow pigments (Fu et al., 2007). To further investigate the mutual regulation between pigments and citrinin metabolism in *M. purpureus* LQ-6, the kinetics of pigments and citrinin biosynthesis were analyzed (Fig. 5C and 5D). According to the experimental results, a small amount of MPs were still detected in SBF of Δ*pig*R with 87.74% production reduced. However, through PCR verification and sequencing analysis (Fig. S3), the *pig*R gene in *M. purpureus* LQ-6 has indeed been completely knocked out. The pigment production after fermentation for 252 h was enhanced by 1.14-fold (from 107.10 U/mL to 121.83 U/mL, or calculated as 2945 U) after deletion of the gene *pks*CT, but almost no citrinin was produced. However, the concentration of citrinin was dramatically increased by 2.03-fold (from 1.85 mg/L to 3.75 mg/L, or calculated as 0.38 mg) that produced by the wild-type strain *M. purpureus* LQ-6 after disruption of the pigment biosynthetic pathway. These results state that different *Monascus* strains may exist differences after disruption of the same gene, this may be also the reason why *M. purpureus* Δ*pig*R constructed in this study still produced pigments. In addition, citrinin and MPs biosynthesis share the same starting unit (acetyl-coA) and extending unit (malonyl-coA) (Hajjaj et al., 1999). The disruption of MPs biosynthesis pathway can increase the production of citrinin, which may be due to more initial and extension units for citrinin biosynthesis. This illustrated that blocking of citrinin or pigment biosynthesis could significantly cause a change in their production in *M. purpureus*, and there is a mutual regulation between pigment and citrinin metabolism.

MPs biosynthesis involves the polyketide synthesis pathway and fatty acid synthesis pathway, in which many NADH/NADPH-dependent redox enzymes are involved. It's speculated that intracellular cofactors metabolism would be disrupted after deletion of genes *pig*R and *pks*CT. Recombination strain *M. purpureus* Δ*pig*CT had the highest pigment production, because the energy used to synthesize citrinin supports the pigment biosynthesis pathway, thereby promoting disruption of the pigment production of *pks*CT. The kinetics analysis of pigment and citrinin biosynthesis showed logarithmic prophase of fermentation of secondary biosynthesis at 96 h (Fig. 5C and 5D). In this phase, a large amount of energy and reducing power are needed to transport the intracellular nutrients to promote the synthesis of metabolic intermediates and support cell growth (Huang et al., 2017). Additionally, the biosynthetic pathway of pigments demands more primary metabolites, such as NADH, NADPH, acetyl-CoA, and malonyl-CoA (Huang et al., 2017; Hu et al., 2012). As shown in Table 1, the level of intracellular NADH and NADPH was sharply decreased by 1.58-fold and 3.71-fold compared to that in the wild-type strain LQ-6 in recombination strain *M. purpureus* Δ*pks*CT at 4 days, respectively, and just slightly enhanced by 1.05-fold and 1.22-fold in *M. purpureus* Δ*pig*R. The concentration of NADH was almost equal between recombinants and parent strain LQ-6 at 6 days (the stationary phases of cell growth, and the logarithmic phase of pigment biosynthesis), but the concentration of NADPH was significantly reduced, especially to *M. purpureus* Δ*pks*CT (reduced by 81.97%). This indicates that deletion of gene *pks*CT can significantly reduce the concentration of NADH and NADPH, especially NADPH, and disrupting the gene *pig*R slightly affects cofactors metabolism. Based on the analysis of metabolic pathways of pigments and citrinin (Fig. 1), hexketide used in the biosynthesis of citrinin was accumulated after deletion of gene *pks*CT, promoting more hexketide chromophores to synthesize pigments with more NADPH and NADH consumption, resulting in low concentrations of NADH and NADPH in *M. purpureus* Δ*pks*CT at fermentation prophase (seen the data of 2 days and 4 days in Table 1), and reducing the growth rate. It may be that the reducing energy originally used for pigment synthesis in *M. purpureus* Δ*pig*R flows to the citrinin synthesis pathway, solving the feedback inhibition of pigment on growth after disruption of pigment biosynthesis. Additionally, a lot of energy, especially NADPH (directly used for pigment biosynthesis) was used for biomass synthesis pathway (such as fatty acid synthesis pathway and lipid synthesis pathway), resulting in the increased cell growth rate and an almost constant concentration of intracellular NADH and NADPH. These results suggested that cofactors are closely related to the synthesis of secondary metabolites, which provides a strategy for improving pigment production.

In this study, the levels of intracellular cofactor NADPH, NADH, glucose consumption, and cell growth

Table 1 The levels of intracellular NADH and NADPH in submerged batch-fermentation of parent strain *M. purpureus* LQ-6 and the recombination strains

Strains	NADH (nmol/g (wet weight))			NADPH (nmol/g (wet weight))		
	2 days	4 days	6 days	2 days	4 days	6 days
M. purpureus LQ-6	1.47 ± 0.11	4.68 ± 0.10	6.04 ± 0.11	1.45 ± 0.07	0.89 ± 0.06	0.61 ± 0.04
M. purpureus Δ*pig*R	1.72 ± 0.12	4.93 ± 0.13	6.88 ± 0.15	1.47 ± 0.09	1.09 ± 0.07	0.89 ± 0.05
M. purpureus Δ*pks*CT	1.19 ± 0.08	2.96 ± 0.05	5.99 ± 0.17	1.29 ± 0.05	0.24 ± 0.03	0.11 ± 0.02
M. purpureus Δ*pks*CT:*pig*R	1.55 ± 0.05	3.13 ± 0.07	6.17 ± 0.14	1.35 ± 0.06	0.72 ± 0.05	0.52 ± 0.03

were disturbed to varying degrees after deletions of gene *pig*R and *pks*CT, as well as the morphology of mycelium. There is a mutual regulation effect between the production of secondary metabolites and mycelial morphology in submerged fermentation by *M. purpureus*. In conclusion, this study improves our understanding of the relationship between secondary metabolites and morphology in *M. purpureus* and provides a strategy for maintaining high MPs production for foods and pharmaceutical fields.

Acknowledgements The authors would like to thank Prof. Tiangang Liu from Wuhan University, China, for kindly providing the pXS plasmid for cloning selection marker G418 fragment and Prof. Feng Yu from Hunan University, China, for kindly providing *A. tumefaciens* EHA105.

Funding This work was supported by National Natural Science Foundation of China (Grant No. 31571874); 2011 Collaborative Innovation Center of Hunan province (2013, No. 448); Natural Science Foundation of Hunan Province (No. 2018JJ3872); Natural Science Foundation of Hunan Province (No. 2018JJ2672); Key Laboratory of Staple Grain Processing, Ministry of Agriculture and Rural Affairs of the People's Republic of China (No. DZLS201706); Research and Development Plan in Key Areas of Hunan Province (No. 2019NK2111); and Natural Science Foundation of Hunan Province (No. 6082019JJ40542).

Compliance with ethical standards

Conflict of interest None of the authors of this study has any financial interest or conflict with industries or parties.

References

Balakrishnan B, Karki S, Chiu SH, Kim HJ, Suh JW, Nam B, Yoon YM, Chen CC, Kwon HJ. Genetic localization and in vivo characterization of a *Monascus* azaphilone pigment biosynthetic gene cluster. Appl. Microbiol. Biotechnol. 97: 6337-6345 (2013)

Chen YP, Tseng CP, Chien IL, Wang WY, Liaw LL, Yuan GF. Exploring the distribution of citrinin biosynthesis related genes among *Monascus* species. J. Agric. Food Chem. 56: 11767-11772 (2008)

Chen G, Bei Q, Huang T, Wu ZQ. Tracking of pigment accumulation and secretion in extractive fermentation of *Monascus anka* GIM 3.592. Microb. Cell Fact. 16: 172 (2017)

Chen G, Wang MH, Tian XF, Wu ZQ. Analyses of *Monascus* pigment secretion and cellular morphology in non-ionic surfactant micelle aqueous solution. Microb. Biotechnol. 11: 409-419 (2018)

Fu GM, Xu Y, Li YP, Tan WH. Construction of a replacement vector to disrupt pksCT gene for the mycotoxin citrinin biosynthesis in *Monascus aurantiacus* and maintain food red pigment production. Asia Pac. J. Clin. Nutr. 16 Suppl 1: 137-142 (2007)

Hajjaj H, Klaébé A, Loret MO, Goma G, Blanc P, Francois JM. Biosynthetic pathway of citrinin in the filamentous fungus *Monascus ruber* as revealed by ^{13}C nuclear magnetic resonance. Appl. Environ. Microb. 65: 311-314 (1999)

Hu ZQ, Zhang XH, Wu ZQ, Qi HS, Wang ZL. Export of intracellular *Monascus* pigments by two-stage microbial fermentation in nonionic surfactant micelle aqueous solution. J. Biotechnol. 162: 202-209 (2012)

Huang T, Tan HL, Lu FJ, Chen G, Wu ZQ. Changing oxidoreduction potential to improve water-soluble yellow pigment production with *Monascus ruber* CGMCC 10910. Microb. Cell Fact. 16: 208 (2017)

Ibrahim D. Effect of agitation speed on the morphology of *Aspergillus niger*HFD5A-1 hyphae and its pectinase production in submerged fermentation. World J. Biol. Chem. 6: 265 (2015)

Jia XQ, Xu ZN, Zhou LP, Sung CK. Elimination of the mycotoxin citrinin production in the industrial important strain *Monascus purpureus* SM001. Metab. Eng. 12: 1-7 (2010)

Kim D, Ku S. Beneficial effects of *Monascus* sp. KCCM 10093 pigments and derivatives: A mini review. Molecules. 23:98 (2018)

Kim HJ, Kim JH, Oh HJ, Shin CS. Morphology control of *Monascus* cells and scale-up of pigment fermentation. Process Biochem. 38: 649-655 (2002)

Kwon HJ, Balakrishnan B, Kim YK. Some *Monascus purpureus* genomes lack the Monacolin K biosynthesis locus. J. Appl. Biol. Chem. 59: 45-47 (2016)

Lai Y, Wang L, Qing L, Chen FS. Effects of cyclic AMP on development and secondary metabolites of *Monascus ruber* M-7. Lett. Appl. Microbiol. 52: 420-426 (2011)

Kim HJ, Ji GE, Lee I. Natural occurring levels of citrinin and Monacolin K in Korean *Monascus* fermentation products. Food Sci. Biotechnol. 16: 142-145 (2007)

Lin L, Wu SF, Li ZJ, Ren ZY, Chen MH, Wang CL. High expression level of mok E enhances the production of Monacolin K in *Monascus*. Food Biotechnol. 32: 35-46 (2018)

Liu J, Guo T, Luo YC, Chai XY, Wu JY, Zhao W, Jiao PF, Luo FJ, Lin QL. Enhancement of *Monascus* pigment productivity via a simultaneous fermentation process and separation system using immobilized-cell fermentation. Bioresour. Technol. 272: 552-560 (2019)

Lv J, Zhang BB, Liu XD, Zhang C, Chen L, Xu GR, Cheung PCK (2017) Enhanced production of natural yellow pigments from

Monascus purpureus by liquid culture: The relationship between fermentation conditions and mycelial morphology. J. Biosci. Bioeng. 124: 452-458

Ning ZQ, Cui H, Xu Y, Huang ZB, Tu Z, Li YP(2017) Deleting the citrinin biosynthesis-related gene, ctnE, to greatly reduce citrinin production in *Monascus aurantiacus* Li AS3.4384. Int. J. Food Microbiol. 241: 325-330

Papagianni M. Fungal morphology and metabolite production in submerged mycelial processes. Biotechnol. Adv. 22: 189-259 (2004)

Patakova P. *Monascus* secondary metabolites: production and biological activity. J. Ind. Microbiol. Biot. 40: 169-181 (2013)

Shao YC, Ding YD, Zhao Y, Yang S, Xie BJ, Chen FS. Characteristic analysis of transformants in T-DNA mutation library of *Monascus ruber*. World J. Microbiol. Biotechnol. 25: 989-995 (2009)

Shao YC, Lei M, Mao ZJ, Zhou YX, Chen FS. Insights into *Monascus* biology at the genetic level. Appl. Microbiol. Biotechnol. 98: 3911-3922 (2014)

Shimizu T, Kinoshita H, Ishihara S, Sakai K, Nagai S, Nihira T. Polyketide synthase gene responsible for citrinin biosynthesis in *Monascus purpureus*. Appl. Environ. Microbiol. 71: 3453-3457 (2005)

Sun XW, Wu HF, Zhao GH, Li ZM, Wu XH, Liu H, Zheng ZM. Morphological regulation of *Aspergillus niger* to improve citric acid production by chsC gene silencing. Bioproc. Biosyst. Eng. 41: 1029-1038 (2018)

Terán HR, de Souza RA, Marcelino PF, da Silva SS, Dragone G, Mussatto SI, Santos JC. Sugarcane bagasse hydrolysate as a potential feedstock for red pigment production by *Monascus ruber*. Food Chem. 245: 786-791 (2018)

Vecht-Lifshitz SE, Magdassi S, Braun S. Pellet formation and cellular aggregation in *Streptomyces tendae*. Biotechnol. Bioeng. 35: 890-896 (1990)

Wang B, Zhang XH, Wu ZQ, Wang ZL. Investigation of relationship between lipid and *Monascus* pigment accumulation by extractive fermentation. J. Biotechnol. 212: 167-173 (2015)

Xie NN, Liu QP, Chen FS. Deletion of pigR gene in *Monascus ruber* leads to loss of pigment production. Biotechnol. Lett. 35: 1425-1432 (2013)

Xie NN, Zhang YP, Chen FS. Identification of a pigment-polyketide synthase gene deleted mutant of *Monascus ruber* M7. Wei Sheng Wu Xue Bao. 55: 863-872 (2015)

Yang XL, Dong Y, Liu GR, Zhang C, Cao YP, Wang CT (2019) Effects of nonionic surfactants on pigment excretion and cell morphology in extractive fermentation of *Monascus* sp NJ1. J. Sci. Food Agric. 99: 1233-1239

Zhang C, Liang J, Yang L, Chai SY, Zhang CX, Sun BG, Wang CT. Glutamic acid promotes monacolin K production and monacolin K biosynthetic gene cluster expression in *Monascus*. AMB Express. 7: 22 (2017)

Zhang K, Yu C, Yang ST. Effects of soybean meal hydrolysate as the nitrogen source on seed culture morphology and fumaric acid production by *Rhizopus oryzae*. Process Biochem. 50: 173-179 (2015)